Flame length of buoyant turbulent slot flame

Article *in* Proceedings of the Combustion Institute · June 2018

DOI: 10.1016/j.proci.2018.05.153

CITATIONS
22

READS
1,327

9 authors, including:

Gao Wei
University of Science and Technology of China
26 PUBLICATIONS **245** CITATIONS
SEE PROFILE

Naian Liu
University of Science and Technology of China
141 PUBLICATIONS **2,695** CITATIONS
SEE PROFILE

Yan Jiao
University of Science and Technology of China
8 PUBLICATIONS **159** CITATIONS
SEE PROFILE

Xisheng Luo
University of Science and Technology of China
230 PUBLICATIONS **3,696** CITATIONS
SEE PROFILE

Available online at www.sciencedirect.com
ScienceDirect
Proceedings of the Combustion Institute 000 (2018) 1–8
Proceedings of the Combustion Institute
www.elsevier.com/locate/proci

Flame length of buoyant turbulent slot flame

Wei Gao [a], Naian Liu [a,*], Yan Jiao [a], Xiaodong Xie [a], Ying Pan [a], Zilong Li [a], Xisheng Luo [a], Linhe Zhang [a], Ran Tu [b]

[a] State Key Laboratory of Fire Science, University of Science and Technology of China, Hefei, Anhui 230026, PR China
[b] College of Mechanical Engineering and Automation, Huaqiao University, Xiamen, Fujian 361021, PR China

Received 30 November 2017; accepted 29 May 2018
Available online xxx

Abstract

This work presents a modeling and experimental analysis on the flame length of buoyant turbulent slot diffusion flame. An approximate predictive correlation of flame length is derived based on the governing equations. The role of initial momentum and buoyancy on flame length is quantitatively described by a modified Froude number Fr_m. The physical model indicates that the flame length of a turbulent slot flame is proportional to $(Fr_m)^{1/3}$ and $(Fr_m)^0$ respectively when the flame is buoyancy-dominated and momentum-dominated. The results, for the first time, give a physical verification on the previous scaling laws on buoyant turbulent slot flame in literature. Slot flame tests are conducted using two burners (for which the width W and length L are respectively 0.9 mm × 20.5 mm and 5.5 mm × 86 mm) and four kinds of high-purity hydrocarbon gas fuels (methane, acetylene, ethane and propane). Experimental data show that the radial temperature profiles of buoyant turbulent slot flames can be well described by a Gaussian function normalized by the temperature radius, which is independent of axial position and flame scale. Moreover, experimental data verify that the physical model applies for different fuel supply rates, types of fuels and flame scales. Additionally, the results indicate that the turbulent slot flame is buoyancy-dominated when $Fr_m < 10^5$, whereas the non-buoyant scenario is approached when $Fr_m > 10^7$. Finally, it is indicated that the scale effect of turbulent slot flame is closely associated with the flame temperature under different flame scales.

Keywords: Flame length; Turbulent diffusion flame; Slot flame; Buoyancy; Physical model

1. Introduction

Diffusion flame from a slot fuel source is of basic and practical importance in fire safety engineering since such kind of flame is frequently encountered in fires. Compared to a general circular pool fire, a slot turbulent flame involves more complex diffusion mechanisms and behaviors due to its significant shear flow, and thus the gas flow of the flame is two-dimensional. This paper is motivated by the need to develop correlations of flame length for buoyant turbulent slot flame. Such correlations are valuable in calculating the radiant energy transmitted from the flame to promote the fire spread over wildland fuels or building flammable wall linings [1–4]. The knowledge on buoyant slot flame

* Corresponding author.
E-mail address: liunai@ustc.edu.cn (N. Liu).

https://doi.org/10.1016/j.proci.2018.05.153
1540-7489

Nomenclature

A	Defined quantity in Eq. (20) (= $T_{st}/T_\infty - 1$) [-]
b	Effective radius [m]
$b_{1/2}$	Temperature radius [m]
fcn	Function [-]
Fr	Initial Froude number (= $u_0^2/(gW)$) [-]
$\mathrm{Fr_m}$	Modified Froude number (= $u_0^2/[\alpha_\rho(1-\rho_{st}/\rho_\infty)gW]$) [-]
g	Gravitational acceleration [m^2/s]
l	Mixing length [m]
L, W	Length/ Width of the slot port [m]
L_f	Flame length [m]
$\dot{Q}$	Heat release rate [kW]
$\dot{Q}_{conv}$	Convective heat flow rate [kW]
r, s	Radial/axial coordinate [m]
Sc	Turbulent Schmidt number [-]
T	Temperature [K]
u, v	Axial/radial velocity of gas [m/s]
v_t	Turbulent eddy viscosity [m^2/s]
x	Defined quantity in Eq. (20) (= $r/(b_{1/2}/\sqrt{\beta_T})$) [-]
y	Defined quantity in Eq. (20) (= $e^x/\sqrt{A}$) [-]
Y	Mass fraction [-]
Z	Mixture fraction [-]

Greek symbols

α_ρ	Empirical coefficient that takes into account the variable gas density in Eq. (8) [-]
β	Proportional constant in Eq. (10) [-]
β_T	Proportional constant related to the radial temperature decay rate in Eq. (18) [-]
ρ	Density [kg/m^3]
φ	Stoichiometric oxygen to fuel mass ratio [-], $\varphi = \upsilon_O \varpi_O / \upsilon_F \varpi_F$
υ	Coefficient in an overall unique reaction [-]
ϖ	Molecular weight [-]
γ	Correction factor in Eq. (13) [-]

Subscripts

CL	Centerline
F	Fuel gas
g	Gas
O	Oxygen
r	Radial
st	Stoichiometric
∞	Infinite
0	Burner surface

Superscripts

$\sim$	Density-weighted mean quantity
–	Time-averaged quantity
$\wedge$	Cross-sectional averaged quantity
$'$	First-order derivative
$''$	Fluctuation of quantity

length is also valuable for determining appropriate safety separation distance in oil and gas industries [5,6].

During the past decades, lots of models and correlations have been developed to describe the flame length of vertical diffusion flames, however, the major attention has been paid to circular flames [7–18]. Roper [19] pioneered a physical model of laminar slot diffusion flame based on the modification of Burke–Schumann theory [20]. A solution of the mixture fraction diffusion equation was obtained by simplifying the axial velocity profile. The thus developed theory, however, does not apply to turbulent slot flame. The early efforts addressing turbulent slot flames were mainly made by Thomas [21] and Yokoi [22]. They introduced a convective heat flux $\dot{Q}_{conv}$ as a scaling parameter based on the Boussinesq approximation and simplified profiles of radial velocity and temperature. An empirical power law based on dimensional analysis, $L_f \propto \dot{Q}_{\mathrm{conv}}^{2/3}$ (L_f is the flame length), was proposed in Thomas [21]. Later, $L_f \propto \dot{Q}^{2/3}$ was suggested for correlating the flame length with different flame scales [23,24].

The literature review reveals some problems that deserve attention. First, the Boussinesq approximation does not apply when a flame involves large density difference, for which, complex flame velocity and temperature profiles may be induced by the significant turbulent mixing with air. In such circumstances, the convective heat flux $\dot{Q}_{\mathrm{conv}}$ or heat release rate $\dot{Q}$ is no longer a conserved scalar in the flame region. Second, the 2/3 power law of slot flame length may not apply for a wide range of $\dot{Q}$. In fact, Hasemi and Nishihata [25] clearly indicated that when $\dot{Q}$ exceeds a certain value, the exponent of the power law would change from 2/3 to 2/5. Third, as noted by Yuan and Cox [24], there is less certainty concerning the constant of proportionality of $L_f \propto \dot{Q}_{\mathrm{conv}}^{2/3}$. So far, only the constants of proportionality of the methane [24] and propane flames [23,25] have been determined. Therefore, a new way of developing prediction models should be explored to determine the constant of proportionality for different types of fuels.

Addressing the above problems, this paper develops a new physical model to predict the flame length for buoyant turbulent slot flame. Based on the governing equations, an approximate predictive correlation of flame length involving a conserved scalar is derived. The role of initial momentum and buoyancy in flame length is quantitatively described and discussed. The correlation is verified by comparing the calculated results with the exper-

Please cite this article as: W. Gao et al., Flame length of buoyant turbulent slot flame, Proceedings of the Combustion Institute (2018), https://doi.org/10.1016/j.proci.2018.05.153

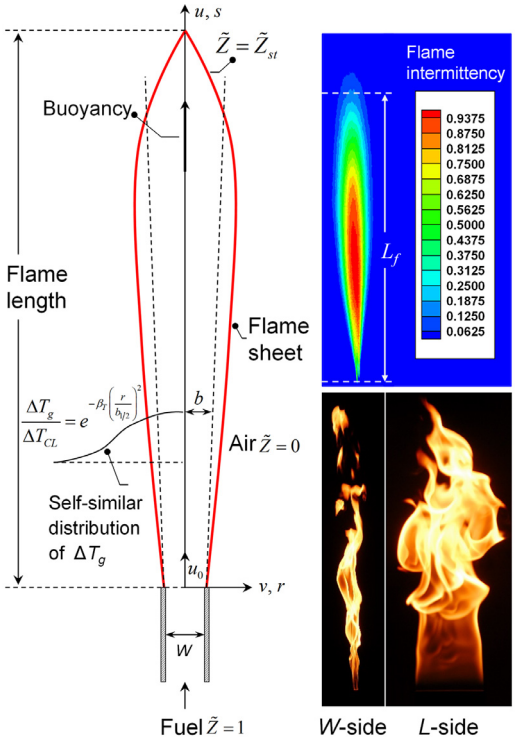

Fig. 1. Schematic of the buoyant turbulent slot diffusion flame, with typical experimental photos (W=5.5 mm, L=86 mm, propane supply velocity: 1.5 m/s).

imental data. The scale effect of the model is also discussed.

2. Flame length model

2.1. Formulation

We consider a turbulent flame vertically issuing from a slot fuel source into still air. The width W and length L of the fuel source satisfy $L > 15\,W$, and thus the fire flow is two-dimensional. The slot flame is depicted in Fig. 1.

The continuity and axial momentum equations are as follows:

$$\frac{\partial}{\partial s}(\bar{\rho}\tilde{u})+\frac{\partial}{\partial r}(\bar{\rho}\tilde{v})=0 \tag{1}$$

$$\bar{\rho}\tilde{u}\frac{\partial\tilde{u}}{\partial s}+\bar{\rho}\tilde{v}\frac{\partial\tilde{u}}{\partial r}=\frac{\partial}{\partial r}\left(\bar{\rho}v_t\frac{\partial\tilde{u}}{\partial r}\right)+(\rho_\infty-\bar{\rho})g \tag{2}$$

here the instantaneous quantity u (axial velocity) or v (radial velocity) is split into a density-weighted mean quantity and a fluctuation, e.g. $u=\tilde{u}+u''$, $\overline{\rho u''}=0$ and $\overline{\rho u}=\overline{\rho\tilde{u}}=\bar{\rho}\tilde{u}$. The tilde and the bar denote the Favre-averaged quantity and time-averaged quantity, respectively. In Eqs. (1–2), ρ is the density, g the gravity acceleration and v_t the turbulent eddy viscosity. The subscript "∞" denotes the infinite. The boundary layer assumption that the radial length scale is much smaller than the vertical length scale is introduced, since the flame is thin and long in shape. Note that the buoyancy is considered in Eq. (2).

Basically, the combustion of a turbulent slot diffusion flame depends on the mixing rate between fuel and oxygen. Thus, the flame structure is described in terms of the mixture fraction (Z) defined as [11]

$$Z=\frac{\varphi Y_F-Y_O+Y_{O,\infty}}{\varphi Y_{F,0}+Y_{O,\infty}} \tag{3}$$

where $\varphi=\upsilon_O\varpi_O/\upsilon_F\varpi_F$, is the stoichiometric oxygen to fuel mass ratio, Y_F and Y_O are the mass fractions of fuel and oxygen, υ_F and υ_O are the coefficients of fuel and oxygen in an overall unique reaction, ϖ_F and ϖ_O are the molecular weights of fuel and oxygen. The subscript "0" denotes the burner outlet surface. The conserved scalar Z varies between 0 and 1. The flame length is defined as the level along the flame centerline where Z equals to the stoichiometric value $Z_{st}=Y_{O,\infty}/(\varphi+Y_{O,\infty})$. For pure fuels mixed with air, Z_{st} is, for instance, 0.055 for CH_4 and 0.060 for C_3H_8. By the boundary layer approximation, the axial diffusion is ignored, and thus the Favre-averaged equation for the mixture fraction is

$$\bar{\rho}\tilde{u}\frac{\partial\tilde{Z}}{\partial s}+\bar{\rho}\tilde{v}\frac{\partial\tilde{Z}}{\partial r}=\frac{\partial}{\partial r}\left(\frac{\bar{\rho}v_t}{\mathrm{Sc}}\frac{\partial\tilde{Z}}{\partial r}\right) \tag{4}$$

where Sc is the turbulent Schmidt number. The boundary conditions are: r=0, $\tilde{v}$ =0, $\partial\tilde{u}/\partial r$ =0,$\partial\tilde{Z}/\partial r$ =0 and $r\to\infty$, $\tilde{u}$ =0, $\tilde{Z}$ =0.

2.2. Approximate solution

Multiplying Eq. (1) by $\tilde{u}$ and combining it with Eq. (2) and Eq. (4), we yield

$$\frac{d}{ds}\int_0^\infty\bar{\rho}\tilde{u}^2dr=\int_0^\infty(\rho_\infty-\bar{\rho})gdr,\ \int_0^\infty\bar{\rho}\tilde{u}\tilde{Z}dr=\rho_0u_0Z_0W/2 \tag{5}$$

The cross-sectional averaged axial velocity ($\hat{u}$) and mixture fraction ($\hat{Z}$) are introduced by

$$\frac{d}{ds}\int_0^\infty\bar{\rho}\tilde{u}^2dr=\frac{d}{ds}\left(\rho_\infty\hat{u}^2b\right),\ \int_0^\infty\bar{\rho}\tilde{u}\tilde{Z}dr=\rho_\infty\hat{u}\hat{Z}b \tag{6}$$

which satisfy that

Please cite this article as: W. Gao et al., Flame length of buoyant turbulent slot flame, Proceedings of the Combustion Institute (2018), https://doi.org/10.1016/j.proci.2018.05.153

$$\tilde{u}, \tilde{Z} = \begin{cases} \hat{u}, \hat{Z} \text{ for } r \le b \\ 0 \text{ for } r > b \end{cases} \tag{7}$$

where b is an area-averaged half-width [11], which differs from the commonly used velocity or temperature radius ($b_{1/2}$) that is defined at the radial location where axial velocity or temperature decays to half the peak value at the same level.

For turbulent buoyant flames, the gas density decreases from ρ_0 at the burner outlet surface to ρ_{st} at the flame length. We introduce an empirical coefficient α_ρ that considers the variable gas density:

$$\int_0^\infty (\rho_\infty - \bar{\rho}) g dr = \alpha_\rho (\rho_\infty - \rho_{st}) g b \tag{8}$$

then combining Eqs. (5–6) we yield

$$\frac{d\left(\rho_\infty \hat{u}^2 b\right)}{ds} = \alpha_\rho (\rho_\infty - \rho_{st}) g b \tag{9}$$

To solve Eq. (9), one needs to find the relationship between db and ds. Since the air is continuously entrained into the slot flame through the turbulent mixing boundary layer, b increases steadily with s. The increase rate of b with time Db/Dt was shown to be proportional to the radial velocity fluctuations v', where D/Dt is the substantial derivative. The Prandtl's mixing length hypothesis gives $v' \sim l\partial\hat{u}/\partial r$, with l being the local mixing length [26]. By assuming $\partial\hat{u}/\partial r \sim \hat{u}/b$ one yields $Db/Dt \sim l\hat{u}/b$. As $Db/Dt = \hat{u}db/ds$, one may further obtain $db/ds \sim l/b$. In free turbulent jet, the mixing length l is known to be proportional to the jet width. Consequently,

$$db/ds = \beta \tag{10}$$

where β is a proportional constant. Now Eq. (9) becomes

$$\frac{d\left(\rho_\infty \hat{u}^2 b\right)}{db/\beta} = \alpha_\rho (\rho_\infty - \rho_{st}) g b \tag{11}$$

With the help of the initial condition $\rho_\infty \hat{u}^2 = \rho_0 u_0^2$, a solution of $\hat{u}$ is obtained:

$$\hat{u}^2 = \frac{\alpha_\rho (\rho_\infty - \rho_{st}) g}{2\beta\rho_\infty} b + \frac{W}{2b\rho_\infty}\left(\rho_0 u_0^2 - \frac{\alpha_\rho(\rho_\infty - \rho_0) g W}{4\beta}\right) \tag{12}$$

Introducing Eq. (12) and Eq. (6) into Eq. (5), we obtain

$$\frac{\rho_\infty W}{2}\left(\rho_0 u_0^2 - \frac{\alpha_\rho(\rho_\infty - \rho_0) g W}{4\beta}\right) b + \frac{\alpha_\rho \rho_\infty (\rho_\infty - \rho_{st}) g}{2\beta} b^3 = \frac{(\rho_0 u_0 Z_0 W/2)^2}{\hat{Z}^2} \tag{13}$$

The area-averaged value $\hat{Z}$ is smaller than the centerline value, as $\hat{u}$ is smaller than the centerline velocity. Therefore, rather than using Z_{st} one should use $\hat{Z} = Z_{st}/\gamma$, where γ is a correction factor for the mixing over the jet area depending on Sc. With the help of the definition of the area-average mass flow rate

$$\int_0^\infty \bar{\rho}\tilde{u} dr = \rho_\infty \hat{u} b \tag{14}$$

γ can be obtained. For slot flames with Sc of 0.5, 0.72 and 1, we obtain that γ respectively equals to 1.57, 1.78 and 2, independent of fuel types and flame scales.

Recall Eq. (10), at the flame length $b = \beta L_f$, then Eq. (13) can be written as

$$\frac{\rho_0}{\rho_\infty \beta}\left(1 - \frac{\alpha_\rho(\rho_\infty - \rho_0)}{4\beta\rho_0 \mathrm{Fr}}\right)\left(\frac{L_f}{W}\right) + \frac{1}{\mathrm{Fr_m}}\left(\frac{L_f}{W}\right)^3 = \frac{(\rho_0 Z_0/\rho_\infty)^2 \gamma^2}{2Z_{st}^2 \beta^2} \tag{15}$$

where the initial Froude number $\mathrm{Fr} = u_0^2/(gW)$, and the modified Froude number $\mathrm{Fr_m}$ is defined as

$$\mathrm{Fr_m} = \frac{u_0^2}{\alpha_\rho(1 - \rho_{st}/\rho_\infty) g W} \tag{16}$$

which denotes the ratio of initial momentum to buoyancy.

2.3. Physical prediction of flame length

In physics, for buoyancy-dominated turbulent slot flame, Eq. (15) predicts that $L_f/W \propto (\mathrm{Fr_m})^{1/3}$. Considering that $\dot{Q} \propto \mathrm{Fr}^{1/2}$ (by rough dimensional analysis), one may deduce that $L_f/W \propto \dot{Q}^{2/3}$, which, for the first time, gives a physical verification on the previous scaling results [23,24]. Besides, Eq. (15) also predicts that for momentum-dominated flame, L_f/W is independent of Fr_m or $\dot{Q}$, as expressed as

$$\frac{L_f}{W} = \frac{\gamma^2}{2\beta}\frac{\rho_0}{\rho_\infty}\left(\frac{Z_0}{Z_{st}}\right)^2 \tag{17}$$

By the data of momentum-dominated flame length, we obtain $\beta = 0.44 \pm 0.01$ for Sc=0.72.

3. Experimental setup

All the experiments were conducted in a test hall (height: 16 m, horizontal dimensions: 9.4 m × 9.4 m) in still air. The experimental setup is depicted in Fig. 2. Slot flames were produced using two stainless-steel gas burners (500 mm in height, wall thickness: 5 mm). The slots of the two burners have cross-sections of 20.5 mm (L) × 0.9 mm (W) and 86.0 mm (L) × 5.5 mm (W) in size, respectively, and thus for both the slot length-to-width ratio is large enough to ignore the three-dimensional effect of flames. The burners were filled with 2 mm diameter glass balls, and two metal mesh layers and

Please cite this article as: W. Gao et al., Flame length of buoyant turbulent slot flame, Proceedings of the Combustion Institute (2018), https://doi.org/10.1016/j.proci.2018.05.153

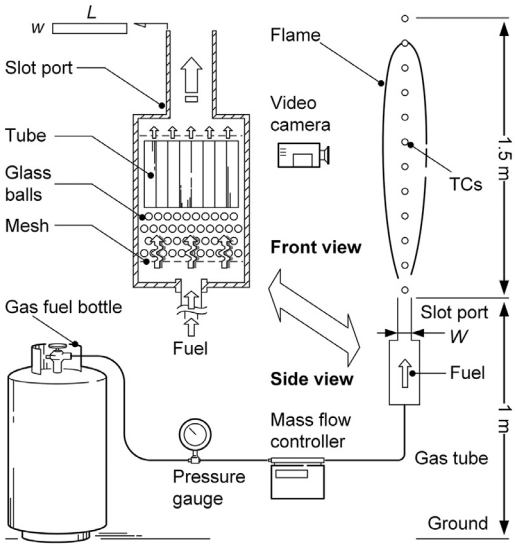

Fig. 2. Experimental design and instrumentations of buoyant turbulent slot diffusion flame tests.

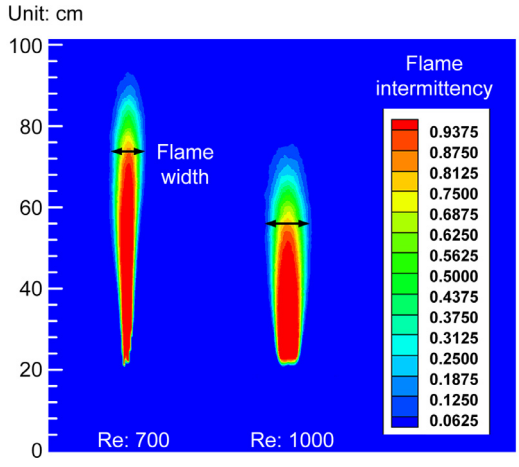

Fig. 3. Intermittency contours of methane slot flame, showing laminar to turbulent transition. (W=0.9 mm, L=20.5 mm, Re: 700 and 1000).

a honeycomb section were used to condition the flow. To obtain a uniform velocity profile, the inside surfaces of the burners were highly polished. In tests, the burner was located on a table which was 1 m from the ground. Four kinds of gas fuels (methane, acetylene, ethane and propane, 97% in purity) were used for tests. The fuel was fed from a gas bottle connected to a pressure gauge. Eleven mass flow controllers (Beijing Sevenstar Electronics Co., Ltd, CS200, calibrated range: 30 L/min for methane, 25 L/min for acetylene, 20 L/min for ethane, 15 L/min for propane) in parallel connection were used to adjust the fuel supply rate with less than 1% of relative errors.

The burning process was recorded by two video cameras (Sony Co. Ltd., FDR-AX100E, 25 frames per second) and a SLR camera (Nikon Co. Ltd., D200, 18–200 mm lens) in the front and side views. Flame images were extracted from the experimental videos. The RGB images were firstly converted into gray scale images and then to the binary images based on the gray scale pixel values and threshold values, thereby the average intermittency for each image frame was determined by imaging processing. The flame length was determined as 50% intermittency height.

The axial and radial flame temperatures were measured by a thermocouple column consisting of K-type thermocouples at thirty axial measuring points with identical intervals. The lowest and highest measuring points were respectively 0.1 m and 1.5 m above the burner outlet surface. An electric displacement platform was used to exactly adjust the horizontal position of the thermocouple column for radial temperature measurement. In each test, temperatures were measured at each radial position for around two minutes. Two thermocouples with bead diameters of 1 mm and 2 mm were used on each measuring position for radiation correction of temperature measurement. The method of radiation correction was consistent with our previous work [27]. Each experiment was performed for at least twice to check the experimental repeatability. By using only one column of thermocouples in each test, the influence of the thermocouples on the flame is considered negligible.

4. Results and discussion

4.1. Experimental observations

The initial Re number at the burner outlet is defined as $u_0 W/v_t$. Figure 3 presents the intermittency contours of a methane slot flame which undergoes laminar to turbulent transition. The transition happens approximately within Re of 500–1000, which, as shown in Fig. 3, is characterized by a remarkable increase of flame width and a decrease of flame length. The flame surface is as well observed to become rougher with coherent structure, associated with the molecular and turbulent mixing processes of the flame. The flame width at the L -side increases very slightly relative to the W-side, which supports the two-dimensional diffusion assumption.

4.2. Radial temperature profile

For turbulent diffusion combustion, when the drawn air reacts with gaseous fuel, the gas temperature decays in radial direction due to air–fuel mixing. Hence, flame length significantly depends

Please cite this article as: W. Gao et al., Flame length of buoyant turbulent slot flame, Proceedings of the Combustion Institute (2018), https://doi.org/10.1016/j.proci.2018.05.153

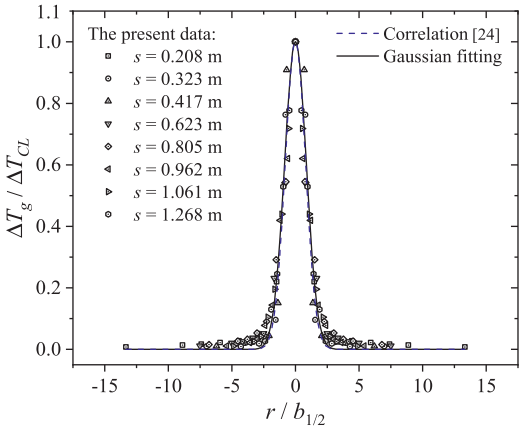

Fig. 4. Gaussian fitting of normalized radial flame temperatures (W=0.9 mm, L=20.5 mm, propane supply velocity: 10 m/s).

on the radial temperature profile of flame. In the present work, we firstly determine the temperature radius $b_{1/2}$ by fitting the data of radial temperatures at each height using a normal Gaussian function [28]. Then we obtain the radial temperature distribution of the flame, for which the excess flame temperature ΔT_g ($= T_g - T_\infty$) is normalized with regard to the excess centerline (CL) flame temperature ΔT_{CL}, and the radial position r is normalized with regard to $b_{1/2}$ at the same level.

As shown in Fig. 4, the normalized radial temperature data at different axial positions (covering the continuous and intermittent flame regions) can be well fitted by the Gaussian function:

$$\Delta T_g/\Delta T_{\mathrm{CL}} = \exp\left(-\beta_T\left(r/b_{1/2}\right)^2\right) \tag{18}$$

This reveals that the radial temperatures at different axial positions have self-similarity. In Eq. (18), β_T is a constant of proportionality related to the radial temperature decay rate, which should have different values for slot flame and circular flame. In this work, we obtain β_T =0.7, which is comparable to Yuan and Cox [24] (β_T =0.78). The slot used by Yuan and Cox [24] (W=15 mm) is one order larger than that used in the present work (W=0.9 mm), and thus it is deemed that the Gaussian profile in the form of Eq. (18) is applicable for a wide range of slot scales. The value of β_T is used to determine the coefficient α_ρ, based on which the flame length can be predicted by Eq. (15).

4.3. Flame length model verification

Figure 5 shows the comparison between the predicted flame length and the experimental data (W=0.9 mm, L=20.5 mm). As shown, for four kinds of hydrocarbon gas fuels (propane, ethane, acetylene and methane), the predicted flame

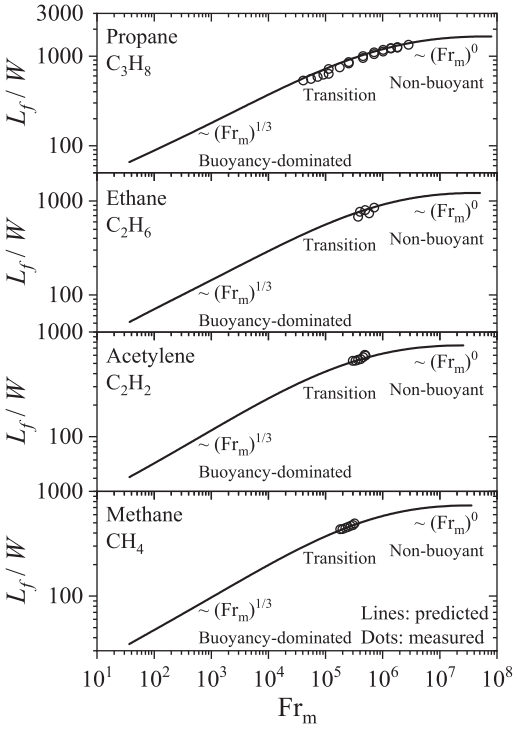

Fig. 5. Comparison of flame length from prediction by Eq. (15) and experiment (W=0.9 mm, L=20.5 mm). The lines and dots are respectively the predicted and measured results.

lengths all agree reasonably well with the experimental data. Especially for propane, the predicted curve completely captures the exponent transition from 1/3 to zero. All the results repeat well. The present physical model is therefore capable of predicting the flame length of different fuel supply rates and is applicable for different types of fuels. As the four kinds of hydrocarbon gas fuels involve alkane and alkyne, we expect that the model and power laws are applicable to many other gas fuels. Besides, in terms of the formulations, the present model also works for gas fuel mixtures (such as LNG or LPG), for which the values of Z_{st} and Z_0 are needed to be calculated by Eq. (3) with knowledge of the mixture components.

Figure 5 also indicates that, for the four kinds of fuels, the slot flames are buoyancy-dominated for $\mathrm{Fr_m} < 10^5$ with 1/3 exponent in the data range, whereas the non-buoyant scenario is approached at least when $\mathrm{Fr_m} \geq 10^7$. For the transition range of $10^5 < \mathrm{Fr_m} \leq 10^7$, the power-law exponent versus $\mathrm{Fr_m}$ should be between 1/3 and zero, which is dependent on the order of $\mathrm{Fr_m}$. This successfully explains the exponent change from 1/3 to 1/5 presented in the work of Hasemi and Nishihata [25].

Please cite this article as: W. Gao et al., Flame length of buoyant turbulent slot flame, Proceedings of the Combustion Institute (2018), https://doi.org/10.1016/j.proci.2018.05.153

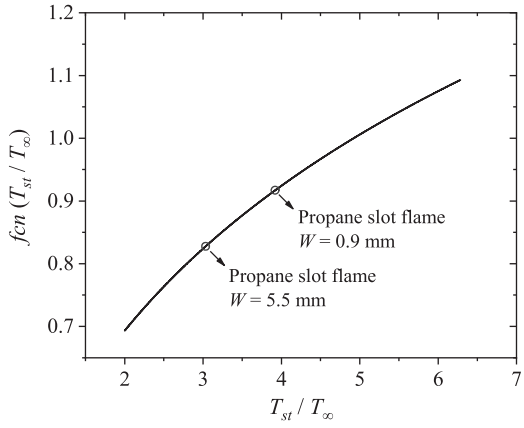

Fig. 6. $fcn(T_{st}/T_\infty)$ versus T_{st}/T_∞ for turbulent buoyant slot flame.

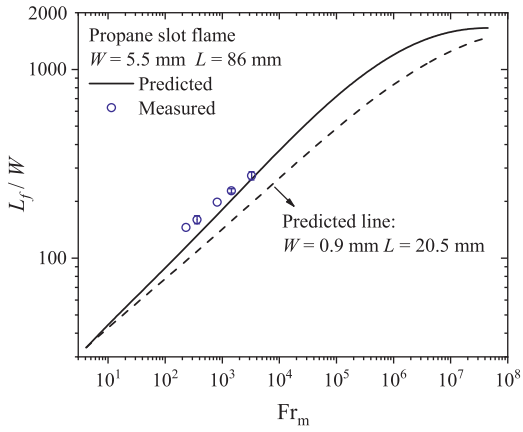

Fig. 7. Comparison of predicted (by Eq. (15) and Eq. (21)) and experimental turbulent flame lengths with slot burner of W=5.5 mm, L=86 mm (fuel: propane).

4.4. Effect of flame scale

A growing interest in fire community is the scaling law of fires, since in many practical scenarios the flame scale can be quite large. Recall in Eq. (15), the quantities ρ_∞, ρ_0, Z_0, Z_{st}, γ and β are the thermo-physical properties of gas fuel, independent of flame scale. Hence, whether L_f/W versus Fr is scale-dependent depends on α_ρ, for which, by applying the ideal gas law to Eq. (8), we obtain $(\bar{\rho}-\rho_\infty)/\rho_\infty \approx (T_\infty - T_g)/T_g$ and $(\rho_{st}-\rho_\infty)/\rho_\infty \approx (T_\infty - T_{st})/T_{st}$, and thus

$$\frac{\rho_\infty - \rho_{st}}{\rho_\infty - \bar{\rho}} = 1 - \frac{T_\infty}{T_{st}} + \frac{T_\infty/T_{st}}{\Delta T_g/\Delta T_{st}} \tag{19}$$

Since $\Delta T_g/\Delta T_{CL} = \exp(-\beta_T (r/b_{1/2})^2)$ and $\Delta T_{CL} = \Delta T_{st}$ at the flame tip, we obtain

$$\int_0^\infty \frac{\rho_\infty - \bar{\rho}}{\rho_\infty - \rho_{st}} dr = \int_0^\infty \frac{1}{(1 - T_\infty/T_{st}) + (T_\infty/T_{st}) \exp\left(\beta_T (r/b_{1/2})^2\right)} dr \tag{20}$$

Let $A = T_{st}/T_\infty - 1$, $x = r/(b_{1/2}/\sqrt{\beta_T})$, and $y = e^x/\sqrt{A}$, the r.h.s. of Eq. (20) thus becomes $(b_{1/2}/\sqrt{\beta_T})(1+1/A)\int_{1/\sqrt{A}}^\infty (y+y^3)^{-1} dy$, which equals to $-(b_{1/2}/\sqrt{\beta_T})(1+1/A)\ln(A+1)/2$. Finally, in the combination of Eq. (8) we obtain

$$\alpha_\rho = \frac{b_{1/2}}{\beta s \sqrt{\beta_T}} \frac{T_{st}}{T_\infty} \frac{\ln(T_{st}/T_\infty)}{2(T_{st}/T_\infty - 1)} \tag{21}$$

Note that $b_{1/2}$ is commonly deemed to be proportional to s, hence $\alpha_\rho \propto s^0$, which indicates that α_ρ is proportional to $(T_{st}/T_\infty)\cdot\ln(T_{st}/T_\infty)/(2(T_{st}/T_\infty - 1))$, which we type as $fcn(T_{st}/T_\infty)$. As shown in Fig. 6, $fcn(T_{st}/T_\infty)$ increases monotonically with T_{st}/T_∞, which implies that for the present model, the scale effect of flames is closely associated with the value of T_{st}/T_∞ under different flame scales.

Basically, with increasing flame scale, the flame may involve significant temperature fluctuation and radiation loss depending on different fuel properties. For a barely sooty flame like hydrogen flames, T_{st}/T_∞ and $fcn(T_{st}/T_\infty)$ may vary little when the flame scale increases. However, for a sooty flame like propane slot flames, as presented in Fig. 6, T_{st}/T_∞ decreases from four to three when W increases from 0.9 mm to 5.5 mm, which may be owing to the significant increase of flame radiation loss. As a result, $fcn(T_{st}/T_\infty)$ and α_ρ vary remarkably, which affects the model calculation.

Case calculations for W=0.9 mm to W=5.5 mm with two different treatments of α_ρ are presented in Fig. 7. The results show that when the variation of α_ρ due to larger flame scale is considered, the predicted curve agrees well with the experimental data, while the predict curve of W=0.9 mm underestimates the data due to the neglect of scale effect. This indicates that for sooty flames like propane flames, the flame scale effect should be considered. However for a specified flame scale, the variation of α_ρ with different fuel supply rates may be neglected based on our observations.

5. Conclusions

This paper presents a modeling and experimental analysis on the flame length of buoyant turbulent slot flame. An approximate predictive correlation of flame length is derived. The role of initial momentum and buoyancy on flame length power law is quantitatively discussed by introducing the modified Froude number Fr_m. The major results are summarized as follows.

(1) The physical model indicates that the flame length of turbulent slot diffusion flame

Please cite this article as: W. Gao et al., Flame length of buoyant turbulent slot flame, Proceedings of the Combustion Institute (2018), https://doi.org/10.1016/j.proci.2018.05.153

is proportional to $(Fr_m)^{1/3}$ for buoyancy-dominated flame and independent of Fr_m for momentum-dominated flame, respectively. The results, for the first time, give a physical verification on the previous scaling laws on buoyant turbulent slot flame in literature.

(2) The radial temperature profile of buoyant turbulent slot flame can be well described by a Gaussian function normalized by the temperature radius, which is independent of axial position and flame scale.

(3) The derived predictive correlation applies for different fuel supply rates, types of fuels and flame scales, which is verified by the experimental data.

(4) Turbulent slot diffusion flame is buoyancy-dominated when $Fr_m < 10^5$, while the non-buoyant scenario is approached at least when $Fr_m \geq 10^7$.

(5) The scale effect of turbulent slot flame is closely associated with the flame temperature under different flame scales.

Acknowledgments

This research is funded by the National Key R&D Program of China (No. 2016YFC0800100) and the National Natural Science Foundation of China (No. 51625602). This work is also supported by the Fundamental Research Funds for the Central Universitiesunder Grants No. WK2320000038 and No. WK2320000036. Wei Gao was supported by the China Postdoctoral Science Foundation (No. 2017M612094).

References

[1] M.A. Delichatsios, *Combust. Sci. Technol.* 39 (1-6) (1984) 195–214.
[2] K. Saito, J.G. Quintiere, F.A. Williams, *Fire Saf. Sci.* 1 (1986) 75–86.
[3] K.M. Tu, J.G. Quintiere, *Fire Technol.* 27 (3) (1991) 195–203.
[4] C. Tsai, D. Drysdale, *Fire Mater.* 26 (6) (2002) 279–287.
[5] N. Gopalaswami, Y. Liu, D.M. Laboureur, B. Zhang, J. Loss, *Prevent. Proc.* 41 (2016) 365–375.
[6] A. Palacios, M. Muñoz, R.M. Darbra, J. Casal, *Fire Saf. J.* 51 (2012) 93–101.
[7] F.R. Steward, *Combust. Sci. Technol.* 2 (4) (1970) 203–212.
[8] H.A. Becker, D. Liang, *Combust. Flame* 32 (2) (1978) 115–137.
[9] T. Gautam, *Combust. Sci. Technol.* 41 (1-2) (1984) 17–29.
[10] E.E. Zukoski, B.M. Cetegen, T. Kubota, *Proc. Combust. Inst.* 20 (1) (1985) 361–366.
[11] N. Peters, J. Göttgens, *Combust. Flame* 85 (1) (1991) 206–214.
[12] M.A. Delichatsios, *Combust. Flame* 92 (4) (1993) 349–364.
[13] J.G. Quintiere, B.S. Grove, *Proc. Combust. Inst.* 27 (2) (1998) 2757–2766.
[14] T.R. Blake, M. McDonald, *Combust. Flame* 94 (4) (1993) 426–432.
[15] J.C. Hermanson, R. Dugnani, H. Johari, *Combust. Sci. Technol.* 155 (1) (2000) 203–225.
[16] A. Palacios, J. Casal, *Fuel* 90 (2) (2011) 824–833.
[17] D. Bradley, P.H. Gaskell, X.J. Gu, A. Palacios, *Combust. Flame* 164 (2016) 400–409.
[18] G. Heskestad, in: M.J. Hurley, D.T. Gottuk, J.R. Hall, K. Harada, E. Kuligowski, M. Puchovsky, J. Torero, J.M. Watts, C. Wieczorek (Eds.), SFPE Handbook of Fire Protection Engineering, Springer, 2016, pp. 396–428.
[19] F.G. Roper, *Combust. Flame* 29 (1977) 219–226.
[20] S.P. Burke, T.E.W. Schumann, *Ind. Eng. Chem.* 20 (10) (1928) 998–1004.
[21] P.H. Thomas, *Proc. Combust. Inst.* 9 (1) (1963) 844–859.
[22] S. Yokoi, Study on the Prevention of Fire-Spread Caused by Hot Upward Current, Report of Building Research Institute No. 34, Ministry of Construction, 1960.
[23] O. Sugawa, H. Satoh, Y. Oka, *Fire Saf. Sci.* 3 (1991) 435–444.
[24] L.M. Yuan, G. Cox, *Fire Saf. J.* 27 (2) (1996) 123–139.
[25] Y. Hasemi, M. Nishihata, *Fire Saf. Sci.* 2 (1989) 275–284.
[26] H. Schlichting, K. Gersten, in: Boundary-Layer Theory, McGraw-Hill, New York, U.S.A., 1979, pp. 300–308.
[27] J. Lei, N. Liu, L. Zhang, et al., *Proc. Combust. Inst.* 33 (2011) 2407–2415.
[28] W. Gao, N. Liu, M.A. Delichatsios, et al., *Combust. Flame* 167 (2016) 409–421.

Please cite this article as: W. Gao et al., Flame length of buoyant turbulent slot flame, Proceedings of the Combustion Institute (2018), https://doi.org/10.1016/j.proci.2018.05.153